

KUCP-0069  
August 1994

# Bounce in Valley: Study of the extended structures from thick-wall to thin-wall vacuum bubbles

HIDEAKI AOYAMA<sup>\*</sup> AND SHINYA WADA<sup>†</sup>

*Department of Fundamental Sciences  
Faculty of Integrated Human Studies  
Kyoto University  
Yoshida, Kyoto 606-01, Japan*

## ABSTRACT

The valley structure associated with quantum meta-stability is examined. It is defined by the new valley equation, which enables consistent evaluation of the imaginary-time path-integral. We study the structure of this new valley equation and solve these equations numerically. The valley is shown to contain the bounce solution, as well as other bubble structures. We find that even when the bubble solution has thick wall, the outer region of the valley is made of large-radius, thin-wall bubble, which interior is occupied by the true-vacuum. Smaller size bubbles, which contribute to decay at higher energies, are also identified.

---

<sup>\*</sup> E-mail address: aoyama@phys.h.kyoto-u.ac.jp

<sup>†</sup> E-mail address: shinya@phys.h.kyoto-u.ac.jp

The decay of the false vacuum can be treated in the imaginary-time path-integral formalism using the bounce solution.<sup>[1,2]</sup> Due to the existence of a negative-eigenvalue fluctuation-mode around the bounce solution, the contour of the gaussian integration through the bounce has to be deformed to yield the imaginary part of the energy level. Thus the decay rate of the false vacuum is obtained.

This bounce belongs to a valley of the action in the whole functional space. This situation is analogous to that of the tunneling processes via instanton, such as the baryon number violation process in the standard model.<sup>[3–5]</sup>

In either cases, when the initial condition is such that the state is in local minimum, the solutions of equations of motion (bounce or instanton) dominates the relevant imaginary-time path integral. However, when the initial state is of higher energy, different configurations could dominate. For the quantum tunneling, the deformed instanton and anti-instanton pair is known to play that role.<sup>[6]</sup> These configuration generally belong to a valley of action, since they form a line of relatively small actions. Initially, streamline method was used to define the valley.<sup>[7–9]</sup> Later, one of the authors (H.A.) and Kikuchi proposed an alternative definition of the valley, the *new valley method*.<sup>[10]</sup> This is obtained by separation of a collective coordinate that corresponds small, zero or negative eigenvalue, which is dangerous for the gaussian integration. In this letter, we employ this new valley method to study the structure of the valley that contains the bounce.

We consider a quantum field theory of a scalar field  $\phi(x)$  in 3+1 dimensional space-time with action  $S$ , which we shall specify later. The new valley equation is given by the following,

$$\int d^4x' D(x, x') \frac{\delta S}{\delta \phi(x')} = \lambda \frac{\delta S}{\delta \phi(x)}, \quad D(x, x') \equiv \frac{\delta^2 S}{\delta \phi(x) \delta \phi(x')}. \quad (1)$$

In the above, the parameter  $\lambda$  is the smallest eigenvalue of the second-order differential operator  $D(x, x')$ . In general, the new valley equation (1) is a fourth-order differential equation for  $\phi(x)$ . We find it convenient to introduce an auxiliary field

to rewrite (1) to a set of two second-order differential equations. This is done in the following manner: The equation (1) can be obtained by varying the following action,

$$S_{\text{NV}} = S + S_\lambda, \quad S_\lambda = -\frac{1}{2\lambda} \int d^4x \left( \frac{\delta S}{\delta \phi(x)} \right)^2 \quad (2)$$

We introduce an auxiliary field  $F(x)$  by adding the following term to the above action, so that the four-derivative term is cancelled out.

$$S_F = \frac{1}{2\lambda} \int d^4x \left( F(x) - \frac{\delta S}{\delta \phi(x)} \right)^2. \quad (3)$$

By varying the total action  $S_{\text{NV}} + S_F$ , we obtain the following equations;

$$\begin{aligned} \frac{\delta S}{\delta \phi(x)} - F(x) &= 0, \\ \int d^4x' D(x, x') F(x') - \lambda F(x) &= 0. \end{aligned} \quad (4)$$

The above set of equations is evidently equivalent to the new valley equation (1). We also note that the solutions of the equations of motion also satisfy the new valley equation with  $F(x) = 0$ .

The Euclidean action  $S$  we study is the following;

$$S = \int d^4x \left[ \frac{1}{2} (\partial_\mu \phi)^2 + V(\phi) \right], \quad V(\phi) = \frac{1}{2} \phi^2 (1 - \phi)^2 - \epsilon (4\phi^3 - 3\phi^4). \quad (5)$$

The above potential has the false minima at  $\phi = 0$  and the true minima at  $\phi = 1$ , regardless of the value of the parameter  $\epsilon (\geq 0)$ . The energy density of the true vacuum is  $-\epsilon$ , even for large  $\epsilon$ . In this sense, this action defines a convenient model for study of thick-wall bubbles as well as thin-wall ones. It should also be noted that any quartic potential can be cast into the above form by suitable rescaling of  $x$  and redefinition of  $\phi$ . In this sense, only the parameter  $\epsilon$  is meaningful. [Especially, the above form is related to that of Ref. 11 by a simple reparametrization.]

As the bounce solution is spherically symmetric, it is most probable that the other configurations in the valley are also spherically symmetric. Thus, we shall confine ourselves to the study of spherically symmetric configurations,  $\phi(x) = \phi(\rho)$  and  $F(x) = F(\rho)$ , where  $\rho \equiv \sqrt{x_\mu^2}$ . The new valley equations (4) then lead to the following;

$$\begin{aligned} \phi'' + \frac{3}{\rho}\phi' - \frac{dV}{d\phi} + F &= 0, \\ F'' + \frac{3}{\rho}F' - \frac{d^2V}{d\phi^2}F + \lambda F &= 0, \end{aligned} \tag{6}$$

where we note the derivatives with respect to  $\rho$  by primes. Just as in Coleman's treatise of the bounce equation, the above equations can be thought as the set of Minkowskian equations of motion of a particle in two dimensional space  $(\phi, F)$  at "time"  $\rho$ . The linear differential terms of  $\phi$  and  $F$  act as friction terms. The other terms are space-dependent forces. The big difference is that now this force is not conservative. Therefore, no simple energy argument is possible.

The New Valley equations (6) require four boundary conditions. They are as follows: For the solution to be regular at the origin  $\rho = 0$ , we require boundary conditions  $\phi'(0) = F'(0) = 0$ . Also, the outside of the bubble has to be the false vacuum, so  $\phi(\infty) = F(\infty) = 0$  have to be satisfied.

In solving (6) numerically, we have chosen to start at the origin with boundary conditions  $\phi'(0) = F'(0) = 0$  and adjust  $\phi(0)$  and  $F(0)$  so that  $\phi(\infty) = F(\infty) = 0$  are (approximately) satisfied. We have done this calculation for  $\epsilon = 0.25$ . The potential for this value of  $\epsilon$  is given in Fig.1. Since the depth of the true vacuum is much more than that of the height of the potential barrier, we expect that the bounce solution is a bubble with thick wall. In Fig.2, we show the numerical solutions. We observe the following in this figure: 1) The new valley contains the bounce solution (broken line). This solution has thick-wall as expected. It has a negative eigenvalue  $\lambda_3$ , which causes the instability. 2) As  $\lambda \rightarrow 0-$ , large bubbles are created. The interior of these bubble is the true vacuum,  $\phi = 1$ . The

latter property is especially notable: Even though the bounce solution is a thick-wall bubble, we find that the valley contains large, thin-wall, clean bubbles in the outskirts.

These thin-wall bubbles can be analyzed by extending the original Coleman's argument: The solution of the new valley equation (6) extremizes the action  $S_{\text{NV}} + S_{\text{F}}$ . Using the first equation of (4), we rewrite it as follows for negative  $\lambda$ ;

$$S_{\text{NV}} + S_{\text{F}} = S + S_{\lambda}, \quad S_{\lambda} = \frac{1}{2|\lambda|} \int d^4x F^2. \quad (7)$$

Now consider a fictitious particle in a one-dimensional space  $\phi$  at time  $\rho$ . In the first equation (6), the auxiliary field  $-F(\rho)$  acts as an “external force” for this particle. If the initial value  $\phi(0)$  is sufficiently close to 1 and  $F$  is sufficiently small,  $\phi$  remains close to 1 for a long time, until the friction term dies away. When it finally rolls down the hill, it does so under the external force  $-F(\rho)$ . If  $-F(\rho)$  is just right, the particle approaches to the top of the lesser hill  $\phi = 0$  asymptotically. Note that there is a major difference with Coleman's argument here: When the roll-down occurs, it does so under the external force, which is the sole source of the energy reduction, while in the bounce solution the timing of the roll-down has to be such that the friction term is just right to take care of the extra energy. [This does not prove the existence of the thin-wall solution, but Fig.2 shows that this in fact happens.] Since  $-F(\rho)$  is the stopping force, it deviates from zero only at the wall. Therefore the second term in (7) contributes positively *only* at the wall. If we denote the radius of the bubble by  $R$ , the actions  $S$  and  $S_{\lambda}$  are approximately written as the following;

$$\begin{aligned} S &= -\epsilon \frac{\pi^2}{2} R^4 + S_1 2\pi^2 R^3, \\ S_{\lambda} &= \frac{W_F}{2|\lambda|} 2\pi^2 R^3, \end{aligned} \quad (8)$$

where  $S_1$  and  $W_F$  are the numbers of  $O(1)$ . Taking the derivative of  $S + S_{\lambda}$  in the above with respect to  $R$ , we find the radius of the solution of the new valley

equation to be

$$R_{\text{NV}} = \frac{3}{\epsilon} \left( S_1 + \frac{W_F}{2|\lambda|} \right). \quad (9)$$

Therefore, even when  $\epsilon$  is not small enough to guarantee the large radius,  $|\lambda|$  can be small enough to do so. This is what is causing the thin-wall bubble to be a solution of the new valley equation.

The shape of the large bubble and its thin wall can be examined in detail by looking at the 0+1 dimensional model, since the friction term can be neglected. We have thus analyzed the 0+1 dimensional model also. We have found that its valley also contains the thin-wall true vacuum bubbles, just as in 3+1 dimensional space-time. We have obtained the numerical value  $W_F \simeq 0.2104$  from this analysis. The radius seen in Fig.2 for  $\lambda_{4,5}$  is in agreement with (9) for this value of  $W_F$ .

Numerical value of the action  $S$  is plotted in Fig.3, where the horizontal coordinate is the “norm” of the solution,  $|\phi| \equiv \sqrt{\int d^4x \phi(x)^2}$ , which for large  $R$  should be  $\sim \sqrt{\pi^2/2}R^2$ . We see in this figure that the bounce solution denoted by its smallest eigenvalue,  $\lambda_3$ , is in fact at the maximum point of the valley. We have also compared the asymptotic expression of action  $S$  in (8) with numerical values of  $S$  for large  $|\phi|$  and have confirmed that the action is in fact dominated by the volume and the surface terms.

On the other side of the valley are small bubbles. In order to see their role, we have calculated the energy  $E$  of the mid-section of bubbles and plotted the result in Fig.4. As is well known, the bubble solution ( $\lambda_3$ ) has  $E = 0$ , so that the energy conservation allows it to contribute to the tunneling from the false vacuum. We find that bubble smaller than the bounce has  $E > 0$ , while larger ones have  $E < 0$ . This shows that the smaller bubble contribute to the tunneling from states with higher energy than the false vacuum.

In summary, we have studied the new valley method and have shown that it is a very powerful tool for the analysis of the structure of the valley. We have numerically examined the valley that contains the bounce solution. We have found

here that even when the bounce solution is a thick-wall bubble, the valley contains thin-wall large bubble, which interior is the true vacuum. Smaller bubbles are also identified and found to contribute to the decay of the higher energy states. This is a rather interesting possibility, which should be explored further. We have also shown in this letter that, unlike the streamline method, the new valley can be obtained from the action  $S_{\text{NV}} + S_{\text{F}}$ . This enables us to calculate valley configurations at given  $\lambda$  with good accuracy either by numerical integration or by variational methods. This method should be useful for other applications of the valley method, such as the tunneling between degenerate vacua. Details of this analysis and further results will be published in near future.<sup>[12]</sup>

## REFERENCES

1. S. Coleman, *Phys. Rev.* **D15** (1977), 2929.
2. C. Callan and S. Coleman, *Phys. Rev.* **D16** (1977), 1762.
3. A. Ringwald, *Nucl. Phys.* **B330** (1990), 1.
4. O. Espinosa, *Nucl. Phys.* **B343** (1990), 310.
5. H. Aoyama and H. Kikuchi, *Phys. Lett.* **247B** (1990), 75; *Phys. Rev.* **43** (1991), 1999; *Int. J. of Mod. Phys.* **A7** (1992), 2741.
6. P. B. Arnold and M. P. Mattis, *Phys. Rev. Lett.* **66** (1991), 13.
7. E.V. Shuryak, *Nucl. Phys.* **B302** (1988), 559; *ibid.* 621.
8. I. I. Balitzky and A. V. Yung, *Phys. Lett.* **168B** (1986), 113; *Nucl. Phys.* **B274** (1986), 475.
9. V. V. Khoze and A. Ringwald, *Phys. Lett.* **B259** (1991), 106.
10. H. Aoyama and H. Kikuchi, *Nucl. Phys.* **B369** (1992), 219.
11. D. E. Brahm and C. L. Y. Lee, *Phys. Rev.* **D49** (1994), 4094.
12. H. Aoyama and S. Wada, Kyoto University preprint, KUCP-0073 (1994).

## FIGURE CAPTIONS

- 1) Potential  $V(\phi)$  for  $\epsilon = 0.25$ .
- 2) Shapes of the solutions of the new valley equation (6). The eigenvalues  $\lambda_{1\sim 5}$  of each lines are  $\lambda_1 = 0.3$ ,  $\lambda_2 = -0.2$ ,  $\lambda_3 = -0.34$ ,  $\lambda_4 = -0.25$ ,  $\lambda_5 = -0.2$ . The broken line shows the bounce solution.
- 3) The action of the solutions of the new valley equation as a function of the norm  $|\phi|$ . The points with eigenvalues  $\lambda_{1\sim 4}$  correspond to the lines in Fig.2.
- 4) The energy of the bubbles at the mid-section, where  $\partial\phi/\partial\tau = 0$ .

This figure "fig1-1.png" is available in "png" format from:

<http://arxiv.org/ps/hep-th/9408156v1>

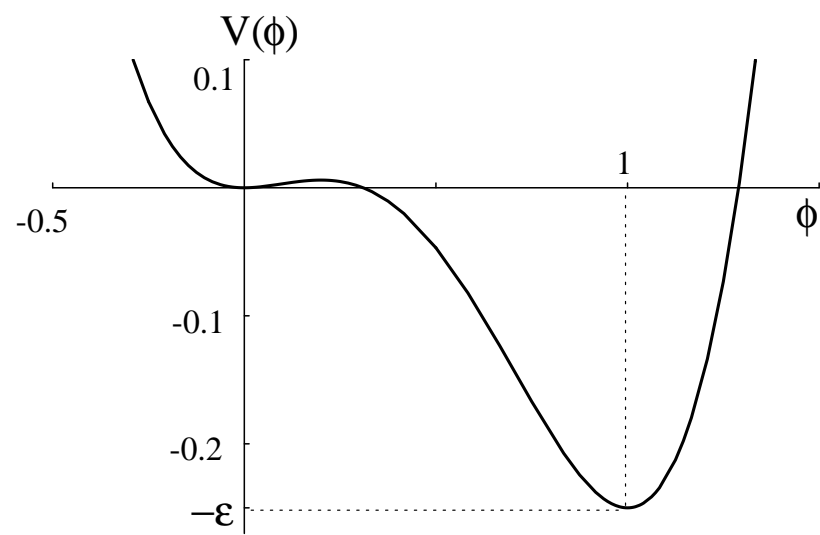


Fig.1

This figure "fig1-2.png" is available in "png" format from:

<http://arxiv.org/ps/hep-th/9408156v1>

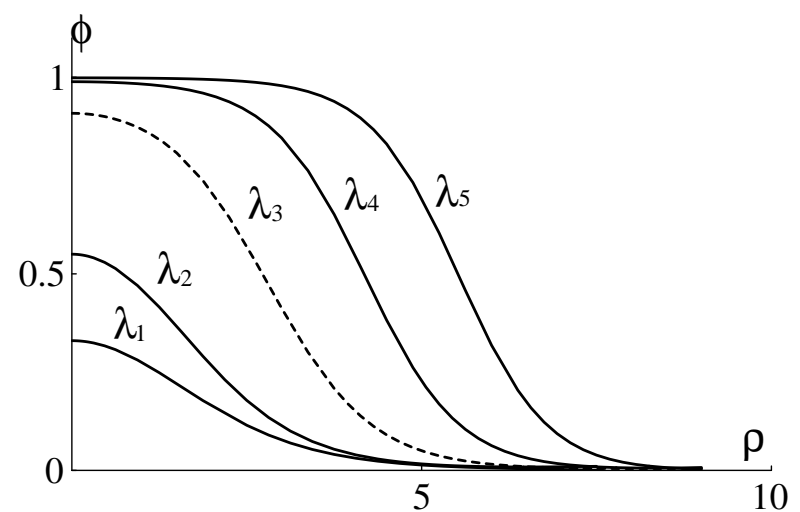


Fig.2

This figure "fig1-3.png" is available in "png" format from:

<http://arxiv.org/ps/hep-th/9408156v1>

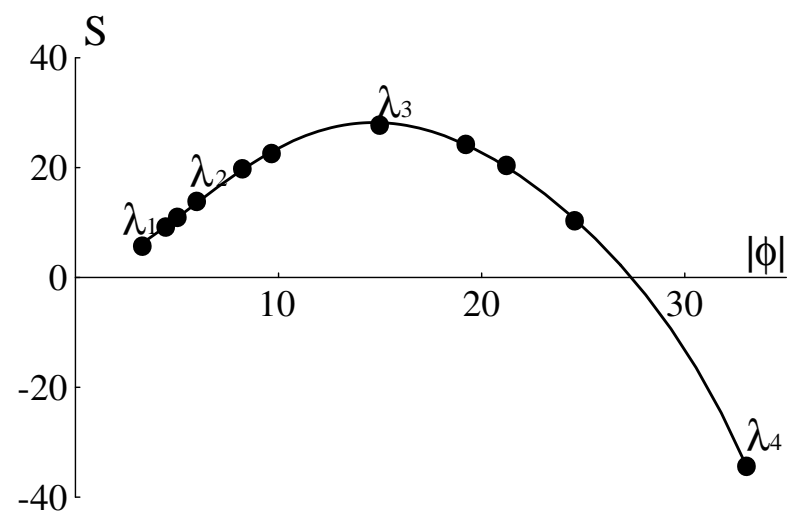


Fig.3

This figure "fig1-4.png" is available in "png" format from:

<http://arxiv.org/ps/hep-th/9408156v1>

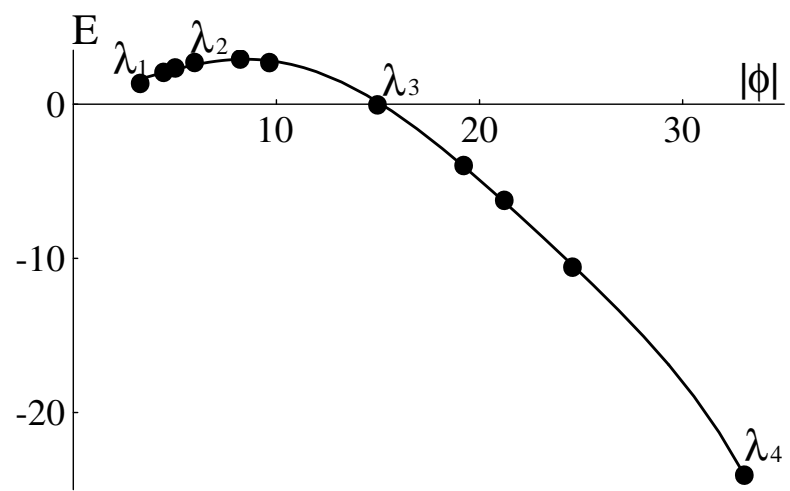


Fig.4